Evaluation of Confocal Microscopy for Measurement of the Roughness of Deuterium Ice

Ryan Menezes

Webster Schroeder High School

Webster, NY

Advisor: Dr. David Harding

Senior Scientist

Laboratory for Laser Energetics

University of Rochester

Rochester, NY

Ryan Menezes

Abstract:

In the direct-drive inertial fusion energy (IFE) concept, fusion targets at around 18 K are rapidly injected into a chamber filled with low-pressure Xe gas at temperatures over 3000 K. In experiments being carried out on OMEGA under the inertial confinement fusion (ICF) program, similar targets are exposed to room temperature conditions prior to being irradiated. Because it is necessary (for both IFE and ICF) that the deuterium (or deuterium-tritium) ice shell within each target remains uniform until implosion, studies characterizing damage to the layer of deuterium fuel are underway. One of these studies plans to use confocal microscopy to obtain 3-dimensional images of the ice before and during heating. In preparation for cryogenic measurements, a confocal microscope has been set up at room temperature to evaluate parameters needed for this study. Several image degradations (arcs, noise, and reflection) have been identified and investigated, and the scan parameters (image size, measurements per second, measurements per pixel, and filter settings) have been optimized for the image clarity of a 40-second scan. These parameters are required for future experiments.

1. Introduction:

In the future, fusion reactions could potentially yield clean and inexpensive electricity. The production of this energy would occur when deuterium (^{2}H) and tritium (^{3}H) react to form a helium atom and a neutron containing 14.1 MeV of energy (^{4}He + ^{1}n) [1]. For the energy in the neutrons to be harnessed to run steam-powered turbines in a profitable power plant, the deuterium and tritium fuel must be contained in targets which can be quickly and rapidly heated and compressed to the intense conditions required for fusion. One method that could achieve these conditions is direct-drive laser-induced inertial confinement fusion (ICF), under which

fusion targets are (in the case of direct-drive) uniformly and directly irradiated with a short laser pulse.

ICF targets contain deuterium vapor within a shell of deuterium ice. (Tritium, which is radioactive, is not usually used in experiments.) Fig. 1 presents the structure of the targets used in OMEGA experiments at the University of Rochester Laboratory for Laser Energetics. The solid deuterium fuel helps achieve the high densities needed for fusion. The targets must be cryogenic, since hydrogen freezes at temperatures below 20 K. Fig. 2 shows that, in comparison to ICF targets, inertial fusion energy (IFE) targets (which are designed for use in power plant situations) are larger and more complex. The ice shells in both targets must remain uniform until implosion, or hydrodynamic instabilities will prevent the target from properly imploding [2].

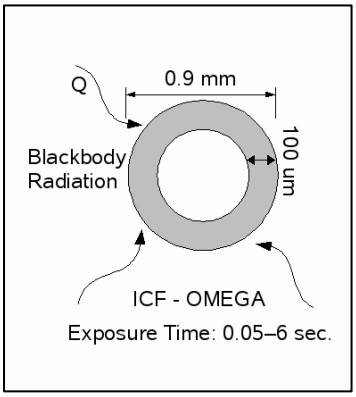

Figure 1: Schematic of a cryogenic target currently used on OMEGA

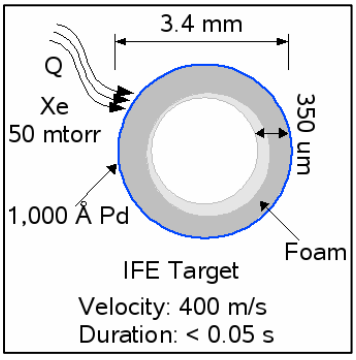

Figure 2: Schematic of a cryogenic target used for inertial fusion energy, injected at 400 m/s through 50 mtorr of Xenon

Both ICF and IFE target designs are subjected to heat fluxes (indicated by the symbol Q in Figs. 1 and 2). ICF targets, which are initially protected by heat shrouds, are exposed to room temperature for 0.05 to 6.0 seconds after the shrouds are removed, and before irradiation [3]. IFE targets, which are shot into the chamber (not placed in it), have a thin palladium layer that reduces blackbody radiation absorbed in the target to insignificant levels. IFE targets experience heat flux from collisions with xenon gas, which protects the chamber walls from the energy created by fusion reactions [4]. The xenon gas is at low pressures, but at very high temperatures (over 3000 °C). In both ICF and

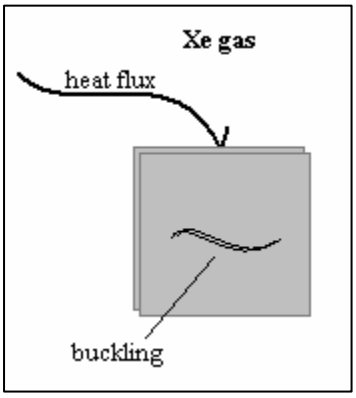

Figure 3: Diagram of buckling in heated Deuterium ice

IFE designs, the heat striking the outside of the target spreads inward, causing the deuterium ice to expand, bend, and buckle (see Fig. 3). It is necessary to understand this buckling in order to create and maintain smooth fusion targets.

Because it is difficult to image the interior of actual targets, a cryogenic setup was earlier designed to simulate heat flow and buckling. Fig. 4 is a schematic of this setup. The entire system is in a vacuum chamber, allowing for control of temperature and pressure. Within the vacuum chamber is a smaller cell, which contains 160 torr of deuterium gas and a confocal microscope (CFM) positioned to image the window at the front of the cell. This window should be cooled to 18.7 K, while the rest of the cell, including the microscope, should reach 91 K. Since the saturated vapor pressure of deuterium gas is 160 torr at 18.7 K, the deuterium condenses and freezes onto the back surface of the window, and not on the rest of the cell or on the microscope, which it could damage. Under the planned future experiment, a jet of hot xenon gas heats the front of the window. Simultaneously, the microscope images the back surface of the ice before and during buckling. A photograph of the smaller cell is shown in Fig. 5.

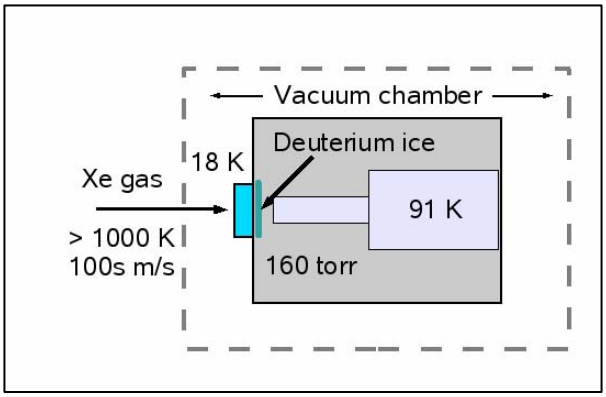

Figure 4: Schematic of the confocal microscope (light blue) within the experimental setup

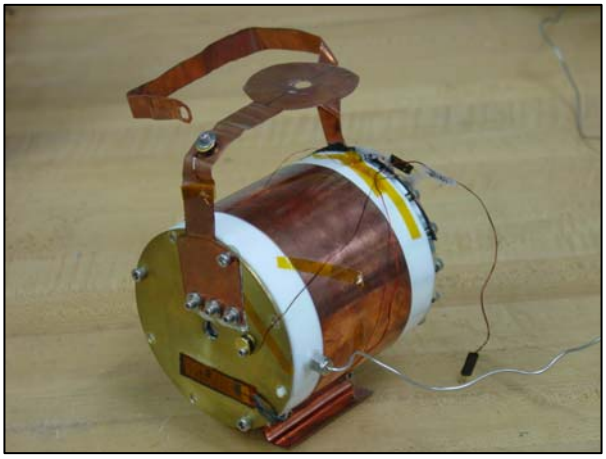

Figure 5: Photograph of the smaller cell of the experimental setup

2. Confocal Microscope:

Fig. 6 illustrates the principle of confocal microscopy. A focused laser beam (red)

illuminates a small point on the sample. The reflected light (green) travels back through the lens. All of the light passing through the lens that originates from the point on the sample enters the end of the optical fiber, while any out-of-focus light does not enter the optical fiber. A detector then measures the in-focus light. (The strength of this signal corresponds to the height of the point on the sample directly below the fiber.) Fig. 7 is a photograph of the microscope that will be used in the planned experiment. The piezoelectric scanner, which can be seen at the bottom of the microscope stack, is a key component of the microscope. Instead of using the scanner to move the sample under the objective, as is traditionally done, this microscope moves the objective over the sample. The scanner's customized placement makes this possible. Fig. 8 shows the scan pattern used by the software that controls the scanner. Directions sent to the scanner cause it to image a line (purple), then image the same line, backward (red), and then step up to the next line (pink) before repeating the process. Note that each of the line scans is composed of steps as small as those between lines, and that readings are taken after each step. After the scan, the scanning software takes the data from the forward lines and combines them to create a forward image, and does the same with the backward lines.

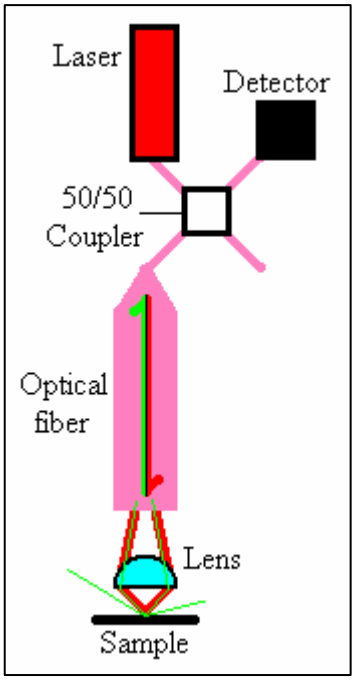

Figure 6: Diagram of the principle of confocal microscopy

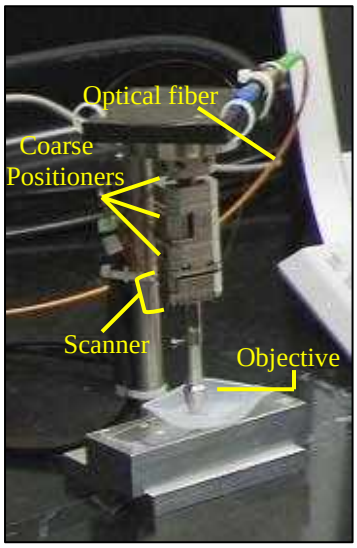

Figure 7: Photograph of the confocal microscope

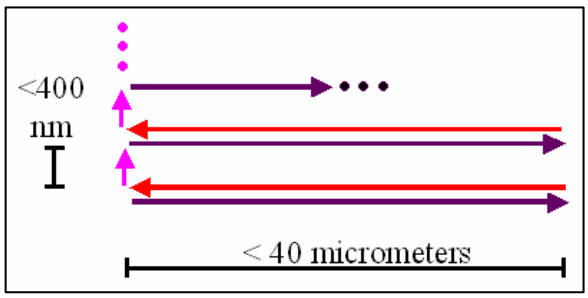

Figure 8: Diagram of the microscope's scan pattern

Basic operation of the microscope comprises 3 steps:

1. Using an oscilloscope, bring the microscope into the focal plane.

   In addition to the scanner, the microscope stack contains three piezoelectric motors for coarse positioning of the objective (see Fig. 7). These motors move in the x, y, and z directions. To find the focal plane, the z motor brings the objective close to the sample (less than 2 mm away). Then, the laser is turned on. The detector sends the return signal to the computer as a voltage, which can be measured using an oscilloscope program. After this program is running, the z motor slowly takes the objective farther away. The voltage return shows a sharp peak at the focal plane, which is approximately 2.9 mm away from the objective.

2. Set the scanning parameters

   Fig. 9 shows a screenshot of AttoScan, the program used to set the scanning parameters and take the image. AttoScan allows the user to change several parameters:

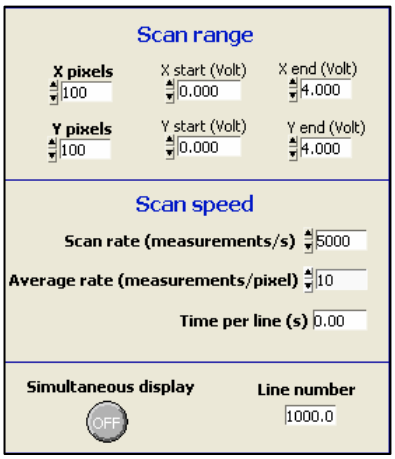

Figure 9: AttoScan screenshot

   - Pixels (Side Length) (Range: 1 to 10,000)
   - Maximum Voltage (Range: 0 to 4) [1]
   - Scan Rate (measurements / s) (Range: 1 to 50,000) [2]
   - Average Rate (measurements / pixel)

   There is also an option to run the current traveling to the scanner through a low-pass filter with a cutoff frequency of 16, 160, or 1600 Hz.

[1] These voltages are amplified 15 times before delivery to the scanner, as are all other voltage values identified.
[2] The CFM manual was unclear. Within this project, the upper bound was considered to be 5,000.

3. Begin the scan

Multiple scans can now be taken without interruption.

3. Experimental Results:

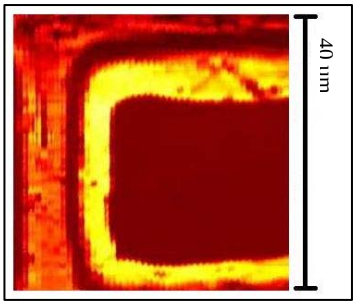

Figure 10: CFM image of a standardized copper grid

The microscope was set up at room temperature for test scans and to identify appropriate scanning parameters. Images were initially taken to illustrate functionality, and to verify the specified scan size of approximately 40 micrometers. Fig. 11 shows images of a piece of copper which was polished with sandpaper, using perpendicular strokes. The diagonal lines, which probably did not result from mechanical effects or from noise, illustrate the functionality of the CFM. Fig. 10 is an image of a copper grid whose dimensions are known. The holes are ~30 micrometers across, while the bars are ~10 micrometers thick. This image verified the specified scan size of approximately 40 micrometers.

Figure 11: CFM image of a polished copper piece

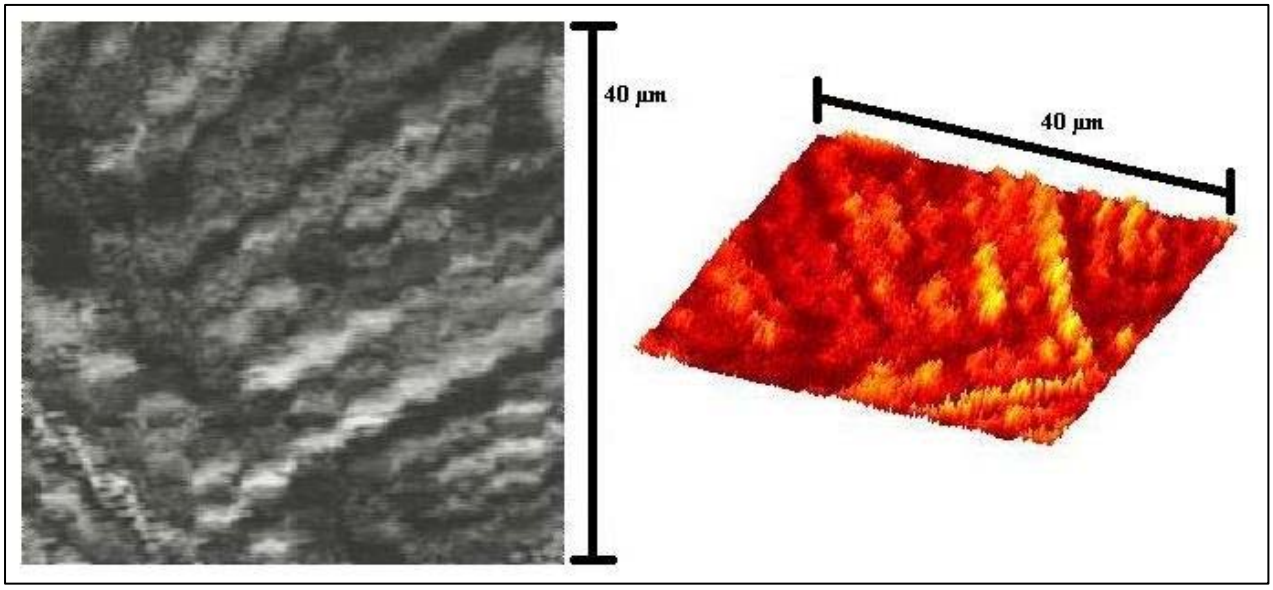

In order to evaluate image quality, standardized scans of an atomic force microscopy (AFM) standard were taken. Fig. 12 illustrates the pattern on this standard and its dimensions. The pitch is 10 µm, and the depth of the pattern is 200 nm. Preliminary scans with this pattern showed several types of image degradation (arcs, "reflection," and noise). In Fig. 13, arc-like distortions are observed, especially on the right side of the image. In Fig. 14, a "reflection" effect is observed on the left side of the image. In Fig. 15, three images were taken of a piece of plastic with small perturbations to show that the reflection is not a real feature. Between each scan, the objective was moved to the left over the sample. As the symmetrical feature in Fig. 15 moves toward the center of the scan area, it becomes evident that it is not actually symmetrical. The reflection effect most probably results from a time lag in the scanning software, which causes the software to add part of the backward image onto the forward image, and part of the forward image onto the backward image. Fig. 16 provides evidence of this explanation.

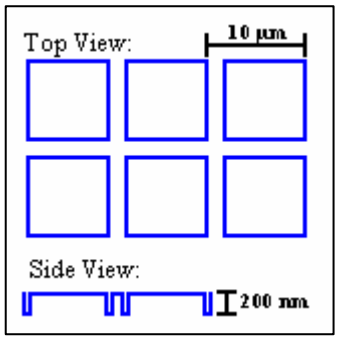

Figure 12: Dimensions of the AFM standard

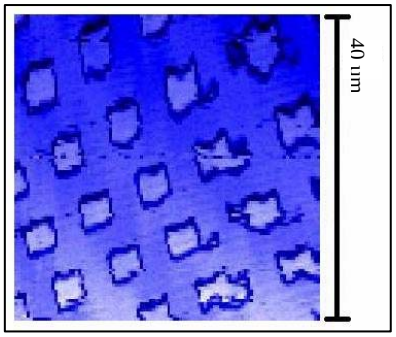

Figure 13: CFM image with arc-like distortions

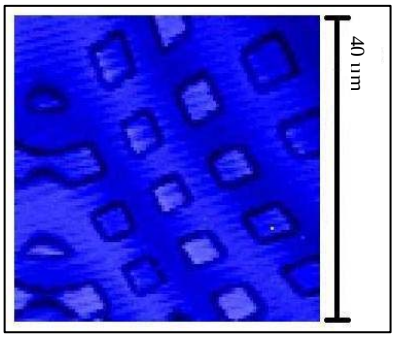

Figure 14: CFM image with the "reflection" effect

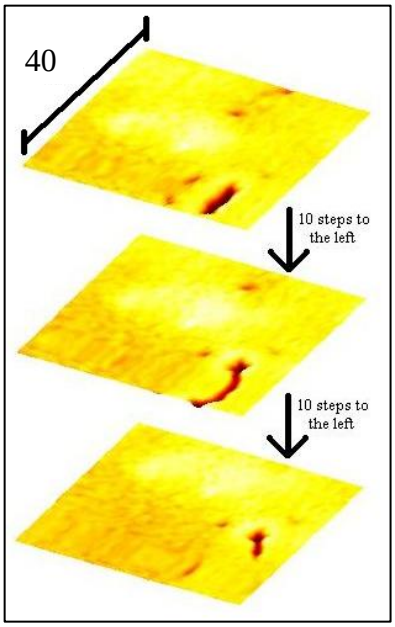

Figure 15: Multiple CFM scans showing that the symmetrical image is not a real feature

The final type of image degradation is observed in Fig. 17, which shows noise in the signal to the detector. Instability in the laser is believed to cause this effect. This belief is based on two facts: First,

the noise in Fig. 17 stops approximately three quarters of the way through the scan, so the scanning parameters are not responsible for the effect; and Second, as Fig. 18 shows, wide and transient variation occurs in the return signal even when no adjustments are made. Nevertheless, there is a possibility that the noise is caused by uncontrolled vibrations.

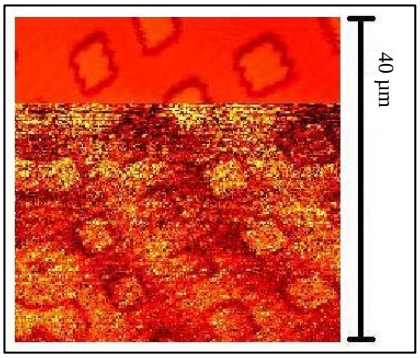

Figure 17: CFM image with noise that stops partway through the scan

The AFM standard shown in Fig. 12 was scanned many times to determine how different scan parameters affect the image.

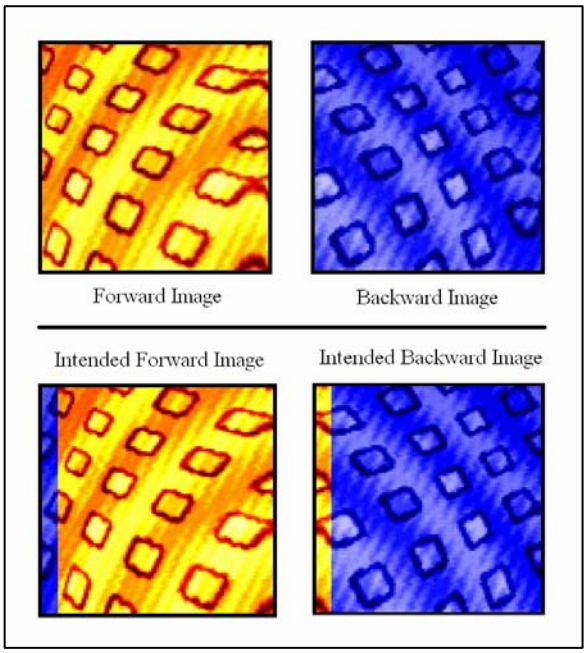

Figure 16: Actual and intended CFM images for forward and backward scans

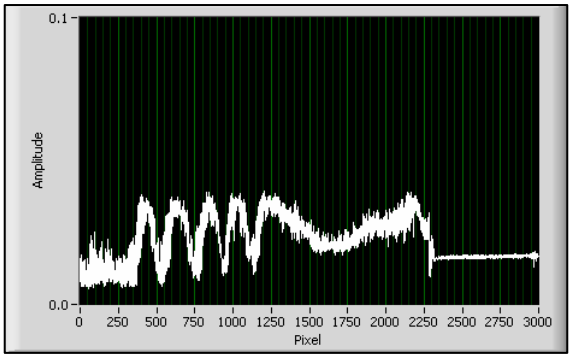

Figure 18: Variation in the CFM's return signal

a) Filter

(16, 160, or 1600 Hz)

Fig. 19 shows that lowering the frequency of the filter reduces the arc effect, while raising the frequency reduces the reflection effect.

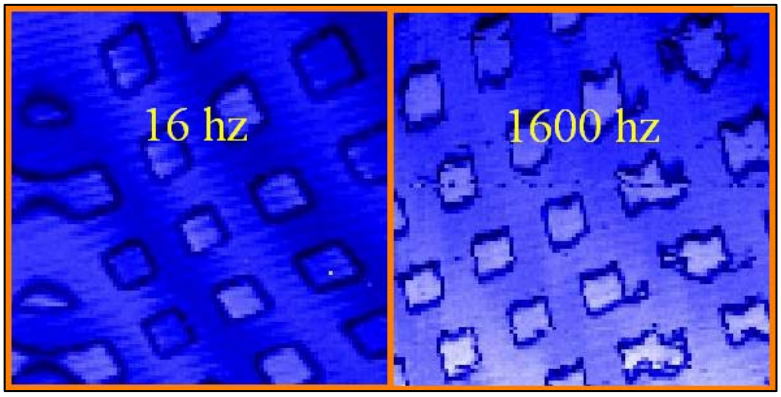

Figure 19: CFM images showing the result of changing the frequency of the filter

b) Pixels (Side Length)

(Range: 1 to 10,000)

Fig. 20 shows that increasing the number of pixels improves image quality by reducing reflection.

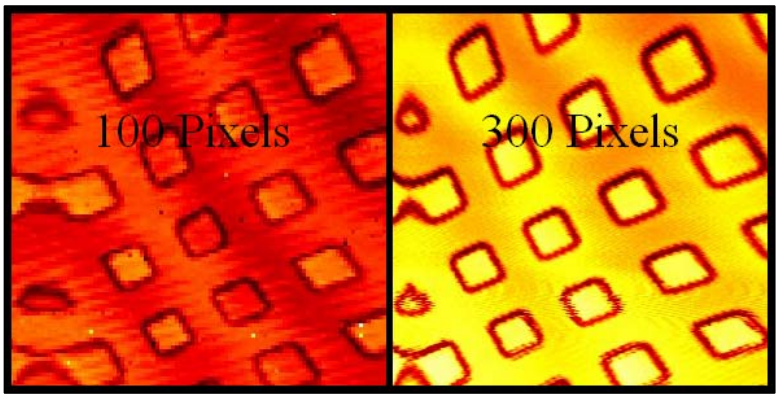

Figure 20: CFM images showing the result of changing the size of the image

c) Maximum Voltage

(Range: 0 to 4)

Fig. 21 shows that decreasing the voltage applied to the piezoelectric scanner decreases the actual dimensions of the scanned image.

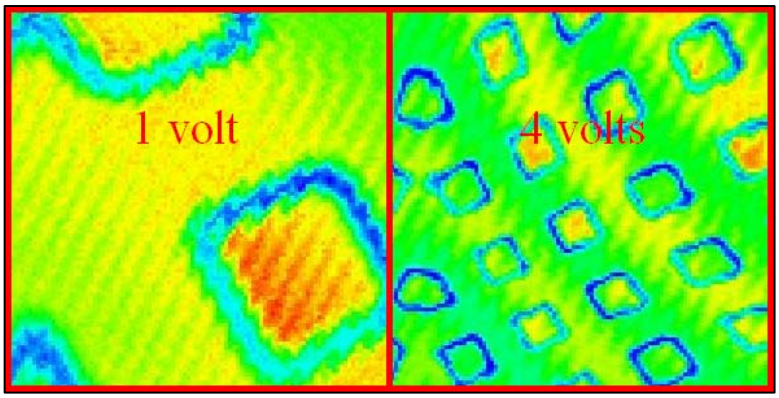

Figure 21: CFM images showing the result of changing the voltage applied to the piezoelectric scanner

d) Scan Rate (measurements / s)

(Range: 1 to 5,000)

Fig. 22 shows that increasing the scan rate increases reflection.

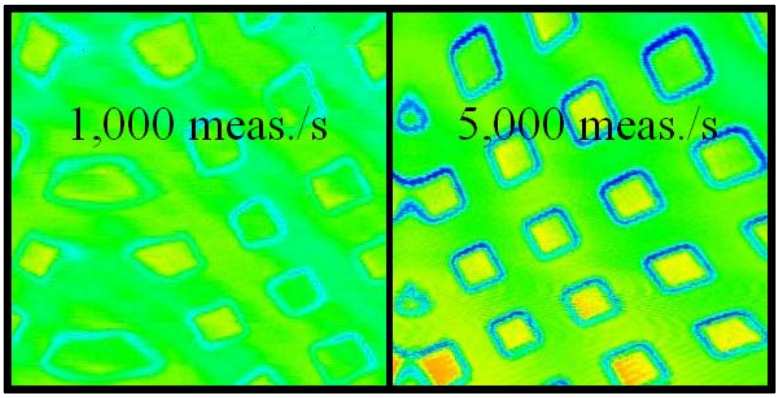

Figure 22: CFM images showing the result of changing the scan rate

e) Average Rate (measurements / pixel)

Fig. 23 shows that increasing the average rate decreases the reflection effect.

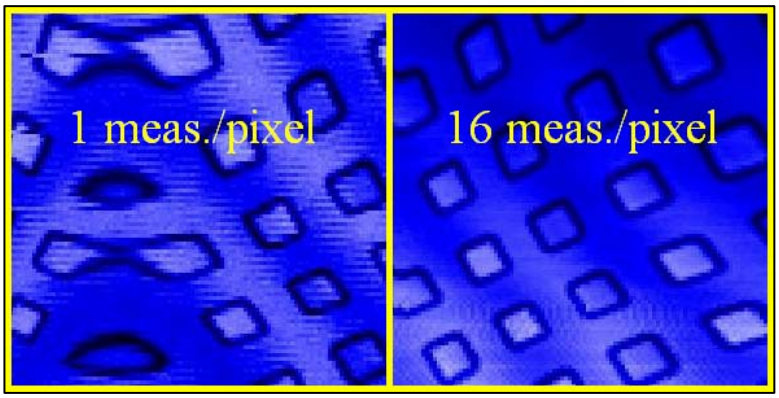

Figure 23: CFM images showing the result of changing the average rate

The time needed to scan an image is given by:

$$Time = (meas.\ per\ pixel) * (pixels\ per\ side)^2 / (meas.\ per\ s)$$

or, $$Time = Average\ Rate * Pixels^2 / Scan\ Rate$$

Since the microscope takes two images per scan (forward and backward), the time must be set to 20 seconds to optimize parameters for a 40-second scan. (The scanning software takes ~8 seconds to prepare before beginning the scan. This added time was ignored.) Based on earlier scans, 100 was determined to be the lowest value for Pixels that still preserved image quality. (Increasing Pixels above 100 increases scanning time quickly because time varies directly with the square of side length.) Under these conditions,

$$20 = Average\ Rate * 100 * 100 / Scan\ Rate,$$

so $$Average\ Rate / Scan\ Rate = 1 / 500.$$

The images in Fig. 24 show that the best image results from the highest average rate, even though this increases the scan rate as well.

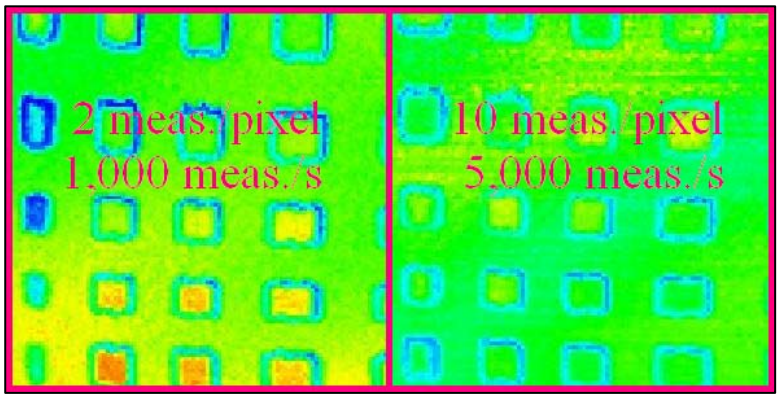

Figure 24: CFM images showing the result of simultaneously changing the scan rate and the average rate

4. Summary:

The effects of different parameters, evident in Figs. 17 through 24 and in other scanned images, are summarized in Fig. 25.

Figure 25: Summary of results

For / Set	Pixels in the X Direction	Filter (Hz)	Measurements per Second	Measurements per Pixel
Fewer Arcs	Higher	Lower	Lower	Higher
Less "Reflection"	Higher	Higher	Lower	Higher
Shorter Scan Time	Lower	~~~	Higher	Lower
40 Second Scan	**100**	**16**	**5,000**	**10**

It was also found that the voltage applied to the piezoelectric scanner, while affecting the scan size, has no noticeable effect on the image quality.

4. Conclusion:

The confocal microscope can demonstrably image a 40 by 40 micrometer area every 40 seconds. The optimal scanning parameters for this time goal are:

- Pixels (Side Length) = 100
- Maximum Voltage = 4
- Filter = 16 Hz
- Scan Rate = 5,000 measurements / s
- Average Rate = 10 measurements / s

The microscope is now ready to be incorporated into the cryogenic setup. The 40-second

scan parameters will be used in the experiment, and the heat flow will be adjusted to accommodate image size and resolution. However, many factors will change at cryogenic temperatures. At low temperatures, more voltage must be applied to the piezoelectric scanner for it to move the same distance, but higher voltages can be applied without causing damage (up to 10 V before amplification). Also, if the noise observed in Fig. 17 is due to vibration, it may disappear at cryogenic temperatures.

Two possibilities which should be explored in the future are the possibility of increasing the Scan Rate past 5,000 (and increasing the Average Rate proportionally) and of replacing the 16 Hz filter with the 1600 Hz filter combined with a computed low-pass filter. Both of these may result in better image quality.

5. Acknowledgements:

Dr. R. Stephen Craxton, without whose invitation I would not have had the opportunity to participate in this program.

Dr. David Harding, who helped me obtain samples to image and whose advice and encouragement improved the project and this report.

Ms Mariana Bobeica, who designed and built the cryogenic setup and who will carry out the planned experiment.

References

[1] V.N. Goncharov, *Basic Principles of Direct Drive Ignition Target Design*, **LLE Review** Vol. 106, p. 83 (2006).

[2] R.W. Petzoldt, *Direct Drive Target Survival During Injection in an Inertial Fusion Power Plant*, **Nuclear Fusion** Vol. 42, p. 1 (2002).

[3] D. Harding, private communication (2007).

[4] D.T. Goodin, et al., *Developing Target Injection and Tracking for Inertial Fusion Energy Power Plants*, **Nuclear Fusion** Vol. 41, p. 527 (2001).